8-1-2021

Gpr37 Modulates Progenitor Cell Dynamics in a Mouse Model of Ischemic Stroke

Sharon Owino
Emory University School of Medicine, sowino@smith.edu

Michelle M. Giddens
Emory University School of Medicine

Jessie G. Jiang
Emory University School of Medicine

Trang Kimberly T. Nguyen
Emory University School of Medicine

Fu Hung Shiu
Emory University School of Medicine

See next page for additional authors

Follow this and additional works at: https://scholarworks.smith.edu/nsc_facpubs

Part of the Neuroscience and Neurobiology Commons

Recommended Citation

Authors

Sharon Owino, Michelle M. Giddens, Jessie G. Jiang, Trang Kimberly T. Nguyen, Fu Hung Shiu, Trisha Lala, Marla Gearing, Myles R. McCrary, Xiaohuan Gu, Ling Wei, Shan P. Yu, and Randy A. Hall

GPR37 modulates progenitor cell dynamics in a mouse model of ischemic stroke

Sharon Owino[1], **Michelle M. Giddens**[1], **Jessie G. Jiang**[1], **TrangKimberly T. Nguyen**[1], **Fu Hung Shiu**[2], **Trisha Lala**[1], **Marla Gearing**[4,5], **Myles R. McCrary**[3], **Xiaohuan Gu**[3], **Ling Wei**[3], **Shan P. Yu**[3,6], **Randy A. Hall**[1]

[1]Department of Pharmacology and Chemical Biology, Emory University School of Medicine, Atlanta, GA 30322, USA;

[2]Department of Human Genetics, Emory University School of Medicine, Atlanta, GA 30322, USA;

[3]Department of Anesthesiology, Emory University School of Medicine, Atlanta, GA 30322, USA;

[4]Department of Pathology and Laboratory Medicine, Emory University School of Medicine, Atlanta, GA 30322, USA;

[5]Department of Neurology, Emory University School of Medicine, Atlanta, GA 30322, USA;

[6]Center for Visual and Neurocognitive Rehabilitation, Atlanta Veterans Affair Medical Center, Decatur, GA 30033, USA

Abstract

The generation of neural stem and progenitor cells following injury is critical for the function of the central nervous system, but the molecular mechanisms modulating this response remain largely unknown. We have previously identified the G protein-coupled receptor 37 (GPR37) as a modulator of ischemic damage in a mouse model of stroke. Here we demonstrate that GPR37 functions as a critical negative regulator of progenitor cell dynamics and gliosis following ischemic injury. In the central nervous system, GPR37 is enriched in mature oligodendrocytes, but following injury we have found that its expression is dramatically increased within a population of Sox2-positive progenitor cells. Moreover, the genetic deletion of GPR37 did not alter the number of mature oligodendrocytes following injury but did markedly increase the number of both progenitor cells and injury-induced Olig2-expressing glia. Alterations in the glial environment were further evidenced by the decreased activation of oligodendrocyte precursor cells. These data reveal that GPR37 regulates the response of progenitor cells to ischemic injury and provides new perspectives into the potential for manipulating endogenous progenitor cells following stroke.

Corresponding author: Randy A. Hall, Department of Pharmacology and Chemical Biology, Rollins Research Center, room 5113, Emory University School of Medicine, Atlanta, GA, 30345. Phone: 404-727-3699. rhall3@emory.edu.

Keywords

GPR37; progenitor cells; gliosis; ischemic injury

INTRODUCTION

Ischemic insults to the central nervous system (CNS), such as stroke, are among the leading causes of disability and mortality worldwide(1). There are currently no effective treatments available to promote recovery and repair in stroke patients. Though functional recovery is limited, prior studies have highlighted the regenerative potential of the central nervous system (CNS) through the activation of endogenous neurogenesis following stroke(2, 3). Classically, the subventricular zone of the lateral ventricle (SVZ) and the sub-granular zone (SGZ) of the hippocampus are the main regions of the CNS known to produce new neurons under both physiological and pathological conditions(3). These regions are enriched in multipotent neural stem/progenitor cells (NSPCs) which reside within the adult CNS, and are increasingly recognized as attractive therapeutic targets(4).

Interestingly, recent studies have demonstrated that NSPCs are located in a number of brain regions other than the SGZ and SVZ (5–9). Notably, following ischemic stroke, NSPCs are localized to the injury zone within the cerebral cortex(10–12) where their maintenance is highly dependent on specific signals within their microenvironment(13, 14). Moreover, recent studies have highlighted that NSPCs function to regulate endogenous neurogenesis following injury in the human brain(15, 16), thereby validating the translational potential of therapeutics targeting these cells. Extrinsic signals such as cell-cell signaling as well as cell-extracellular matrix signaling can regulate various aspects of NSPC physiology and maintenance. Although NSPCs have been identified in the cerebral cortex, this region has generally been classified as an atypical, non-germinal stem cell niche(17). Under baseline conditions, the cerebral cortex is thought to contain committed precursor cells that can self-renew, but are unable to induce comprehensive neurogenesis(18) due to inhibitory extrinsic signals emitted from their microenvironment(19). Currently, the precise molecular cues regulating the dynamics of these cells remain mostly unknown.

GPR37 is a G protein-coupled receptor that is also known as the "parkin-associated endothelin-like receptor" ("Pael-R") and predominantly expressed in the brain(20–22). It is known to be highly expressed in mature oligodendrocytes, where it functions to inhibit oligodendrocyte maturation(20) and decrease susceptibility to demyelination(23). GPR37 can also exert cytoprotective actions in cultured cells(24–26) and modulate susceptibility to Parkinson's disease-like pathology *in vivo* (27–29). We recently identified GPR37 as a key regulator of the CNS response to ischemic stroke-like injury: when GPR37 is deleted in a rodent model, acute ischemic damage is more severe(30). In the present study, we found that GPR37 is dramatically upregulated following focal cortical infarction and functions as a critical negative regulator of progenitor cell dynamics within the cerebral cortex following ischemic injury.

Materials and Methods:

Generation of knock out mice and maintenance of mouse colony

Mice lacking GPR37 ($Gpr37^{-/-}$) were obtained from Jackson Laboratory (strain $Gpr37^{tm1Dgen}$, stock number 005806). This strain contains a bacterial LacZ reporter gene in the Gpr37 locus. To ensure uniformity of genetic background, these mice were backcrossed with wild-type mice (The Jackson Laboratory) for ten consecutive generations. The successful deletion of $Gpr37$ was then confirmed via DNA sequencing and the loss of GPR37 protein expression validated by western blotting brain tissue samples from WT and $Gpr37^{-/-}$ mice with an anti-GPR37 antibody (MAb Technologies). All mice were housed in a 12-hour light/dark cycle with food and water available *ad libitum* and all experiments performed prior to 5:00 pm. Male mice were used for all stroke induction paradigms. All experiments were conducted in accordance with the guidelines of the Institutional Animal Care and Use Committee of Emory University.

Antibodies

The following antibodies were used: rabbit polyclonal to GPR37 (Mab Technologies, WB 1:1000); chicken polyclonal to β-gal (Abcam, ab9361, IHC 1:500) ; mouse monoclonal to CC1(Millipore, OP80, IHC 1:500); rat monoclonal GFAP(Invitrogen,13-0300, IHC 1:500); goat polyclonal to Iba1(Abcam, ab5076, IHC 1:500); mouse monoclonal to NG2 (Santa Cruz, sc 53389, IHC 1:200); rabbit polyclonal to Olig2 (Millipore, AB9610, IHC 1:500); rabbit polyclonal to Sox2 (Stemgent, 09–0024, IHC 1:200); rabbit polyclonal to cleaved Caspase-3 (Cell Signaling Technology, 9661, IHC 1:200). Secondary antibodies were species specific Alexa Fluor 488, Alexa Fluor 568, or Alexa Fluor 647 immunoglobulin G (IgG) (heavy and light chains) (Jackson ImmunoResearch, 1:500).

Focal ischemia stroke model

A sensorimotor cortex ischemic stroke was induced within $Gpr37^{-/-}$, WT littermate controls and C57BL/6 mice (male mice, 2–3 months of age). This paradigm used was induced based on prior reports of barrel cortex stroke with mofified artery occlusion protocols (30, 31). Animals were given ketamine/xylazine (ketamine 80–100 mg/kg i.p., xylazine 10–12.5 mg/kg, i.p.) anesthesia following which the right middle cerebral artery was permanetly ligated (10-0 suture, Surgical Specialities CO, Reading, PA, USA). The production of right sensorimotor ischemia was then followed by bilateral occlusions of the common carotid artery for seven minutes and reperfusion. This modified ischemic procedure resulted in the production of a specific infarct formation within the right sensorimotor cortex.

Before and after surgery, the animals were housed in groups of 5 animals per cage, and allowed access to food and water *ad libitum*. During the surgery and in the recovery phase, animal body temperature was monitored using a rectal probe and maintained at ±37°C by a homeothermic blanket control unit (Harvard Apparatus, Holliston, MA, US) and animals were kept within a ventilated humidity controlled incubator (Thermocare, Incline Village, NV, USA) . Before surgery, animals were given a single dose of meloxicam (oral, 5 mg/kg), followed by daily doses of meloxicam (oral, 5 mg/kg) for three days post-surgery. Following the surgery animals were monitored for 60min to confirm proper recovery from

anesthesia and monitor locomotor activity and animal health. The overall mortality rate for this paradigm was 5%. Mice were sacrificed with an overdose of isoflurane and decapitation three days following stroke. The brains were then immediately removed and transferred to 4% paraformaldehyde or stored at −80°C until further processing. All animal protocols were approved by the Institutional Animal Care and Use Committee (IACUC) of Emory University School of Medicine.

Western blot

Isolated protein samples were reduced and denatured in Laemmli buffer and then analyzed via SDS-PAGE. Samples were loaded onto 4–20% Tris-glycine gels (BioRad) and then subsequently transferred to nitrocellulose membranes (BioRad). For analysis via chemiluminescence, membranes were blocked in 5% milk (5% non-fat milk in 50 mM NaCl, 10 mM HEPES, pH 7.3, 0.1% Tween-20 (Sigma) in ultrapure water) and then incubated shaking overnight at 4°C with primary antibodies. Densitometric protein quantification was performed using ImageJ software.

Immunofluorescence

For immunohistochemistry, brains were removed and postfixed for 24hrs. at 4°C in 4% PFA. The brains were then cryopreserved at 4°C in a solution of 30% sucrose/PBS overnight. From each brain 40μm frozen sections were cut coronally using a freezing microtome. Sections were collected, three per well into 96 well plates containing cryoprotectant solution (*TBS/30% ethylene glycol/15% sucrose/0.05% sodium azide)* and stored at −20°C prior to histological processing. Sections were then washed with PBS, incubated in 1% H_2O_2, washed again with PBS and then blocked for 60 min in a solution containing 1M Tris-Brij 35 (pH 7.5), 0.3% Triton X-100/15% normal goat serum before overnight incubation with specified primary antibody diluted in Tris-Brij 35 (pH 7.5). To make a 1M Tris-Brij solution, Brij 35 (30%) was used to make a final working buffer containing 2.5% Brij 35 in 1M Tris. Sections were then rinsed in Tris-Brij 35(pH 7.5) and incubated for two hours with specified secondary antibodies. In instances where signal amplification was necessary, TSA amplification(32) (Akoya Biosciences) was utilized. For double labeling experiments, a region of tissue known to contain the protein of interest was used as a positive control and tissues incubated in secondary antibodies without primary antibodies present were used as negative controls in the staining protocols. All double-label experiments were done in parallel for incubation of primary antibodies, followed by sequential incubation of secondary antibodies. Anti-mouse AffinPure Fab fragment (Jackson ImmunoResearch) was used to minimize non-specific labelling of mouse primary antibodies used in mouse tissue.

Confocal images were acquired using a Leica SP8 inverted microscope using the LASX unmixing software to obtain z-stack datasets. Three to four sections per mouse were used for immunofluorescence staining. Immunoreactive cells were analyzed within the peri-infarct region utilizing ImageJ software. Cell counting was performed for immunoreactive cells within the peri-infarct region. The 'Sum projection' feature in ImageJ was used to obtain a composite image of multiple z-stacks. Fluorescence intensity was calculated for a region of interest (ROI) within the peri-infarct region. A threshold was determined across all images for each antibody used. The total fluorescence intensity of immunoreactive cells

within the ROI was calculated using the "Measure" feature of ImageJ. All colocalization analyses were performed using ImarisColoc software (Imaris 9.3), which enables processing of three-dimensional microscopy images.

Statistical analyses

Prism 6 *(GraphPad Software, La Jolla, CA, USA)* was used to perform statistical analysis and generate graphical representations. For comparisons between two experimental groups, a two-tailed student's t-test with unequal variance was used. For comparisons between multiple experimental groups, one-way ANOVA and two-way ANOVA were used followed by Holm-Sidak multiple comparisons correction. Mander's overlay coefficient was used to measure the degree of colocalization between specified outputs. Statistical significance was defined as p 0.05. All graphical data are presented as the mean ± SEM.

RESULTS

Gpr37 is upregulated following injury

Given our previous observations that GPR37 regulates key signaling pathways following ischemic injury(30), we assessed the expression levels of GPR37 in mice before and after the middle cerebral artery occlusion (MCAO) model of stroke. Three days following MCAO, Western blot studies revealed that WT mice exhibited a dramatic (~6-fold) increase in GPR37 levels within the peri-infarct region (Figure 1a–b). A depiction of the full immunoblot for Figure 1a is provided in Supplemental Figure A. We next sought to extend these findings using immunohistochemistry, but studies using commercially available anti-GPR37 antibodies failed to yield an antibody that specifically labeled WT brain sections without non-specifically labeling brain sections from *Gpr37*^{−/−} mice. We therefore took advantage of the fact that the GPR37 promoter in *Gpr37*^{−/−} mice contains a bacterial LacZ reporter gene. Detection of β-galactosidse (β-gal) in *Gpr37*^{−/−} sham and MCAO samples revealed a pronounced increase (~3-fold) in β-gal-positive cells surrounding the focal injury (Figure 1c–h), which was consistent with the Western blot data. Thus, findings made using two independent techniques (including both direct and indirect measures) revealed that GPR37 is robustly upregulated within cells in the peri-infarct region following ischemia. Surprisingly, cells expressing β-gal could be visualized within the boundary of the peri-infarct region, as denoted by the boundary of glial fibrillary acidic protein (GFAP)-positive astrocytes, as well as within the ischemic core (Figure 1d). The astrocytes within this region exhibited robust expression of GFAP, consistent with astrocytes that had undergone astrogliosis triggered by the ischemic injury.

Post-stroke GPR37-positive cells are not mature oligodendrocytes

We next addressed the identity of the cell population in which GPR37 was upregulated following ischemic injury. In uninjured brain tissue, GPR37 is most abundantly expressed in mature oligodendrocytes within white matter regions such as the corpus callosum, hippocampal fimbria, and caudate putamen(20, 23) (Supplemental Figure B). To determine if the large population of GPR37-positive cells in the cortex following focal injury were oligodendrocytes, we performed immunohistochemical labeling on brain tissue from *Gpr37*^{−/−} mice (sham vs. MCAO) to assess colocalization between β-gal (indicating

GPR37 expression) and adenomatous polyposis coli clone CC1, a marker for mature oligodendrocytes. These studies revealed that approximately 80% of β-gal-positive cells were CC1-positive (Figure 2a–d, k) in sham brains, suggesting that these cells are mature oligodendrocytes. In contrast, studies examining the peri-infarct region of MCAO brain tissue revealed that only about 15% of β-gal-positive cells colocalized with CC1 (Figure 2f–j, k). In the stroke tissue, many CC1-positive cells following ischemia corresponded to reactive astrocytes, as visualized with GFAP staining (Supplemental Figure C), and consistent with previous reports[33]. However, the clear majority of β-gal-positive cells were not CC1-positive (Figure 2f–k), indicating that these cells were neither mature oligodendrocytes nor reactive astrocytes.

Indeed, the β-gal-positive cells that we observed so abundantly after MCAO did not colocalize with any classical reactive glia markers (Figure 3a–d). β-gal staining did not colocalize (% colocalization   10%) with the reactive astrocyte marker GFAP (Figure 3a), the reactive oligodendrocyte progenitor cell (OPC) marker NG2 (Figure 3c) or the reactive microglia marker IBA1 (Figure 3b). However, β-gal staining did exhibit robust colocalization (~80%) with Olig2 following MCAO (Figure 3e–g). Interestingly, while 80% of β-gal positive cells were immunoreactive for Olig2, only about 55% of total Olig2-positive cells were immunoreactive for β-gal (Figure 3f). Mander's overlap coefficient was used to further quantify the degree of colocalization between β-gal and Olig2. For total β-gal-positive cells immunoreactive for Olig2, the Mander's coefficient was 0.91±0.03, whereas for total Olig2-positive cells immunoreactive for β-gal the coefficient was 0.56±0.07. Olig2 is known to be expressed in oligodendrocyte lineage cells[34–36] but also known to be expressed more broadly in progenitor cell populations[37–39]. To rule out the possibility that these cells represented a population of cells undergoing apoptosis, we assessed colocalization between β-gal and cleaved caspase-3 (Supplemental Figure D) and found that β-gal-positive cells did not express this marker for active cell death. Additionally, these cells did not express the migratory neuroblast marker DCX (Supplemental Figure E). Taken together, these data suggest that 3 days following experimental ischemic stroke, GPR37 is highly expressed by viable Olig2-positive cells that are not mature oligodendrocytes.

The large increase in β-gal-positive cells observed after MCAO in *Gpr37*$^{-/-}$ mice, coupled with the observation that most of these β-gal-positive cells were positive for Olig2, suggested that there must be an overall increase in the number of Olig2 expressing cells in the peri-infarct region following ischemic injury. We tested this idea in the experiments illustrated in Figure 4. Following MCAO in *Gpr37*$^{-/-}$ mice, we observed a significant increase in Olig2-positive cells in the peri-infarct region, consistent with the findings described above (Figure 4f,h). Interestingly, this observation only held true for the brain tissue from the *Gpr37*$^{-/-}$ mice (Figure 4f): in brain sections from WT mice, Olig2-positive staining was not increased after MCAO, and in fact tended to decrease (Figure 4e,g).

Gpr37 is upregulated in Sox2-positive progenitor cells, which exhibit altered responses in *Gpr37*$^{-/-}$ mice

Several studies have highlighted the role of Olig2 in the regulation of stem/progenitor cell fate(38, 40). Since GPR37 colocalized with Olig2 but not with mature glial cell markers, we examined whether these cells expressed other markers for stem or progenitor cells. Surprisingly, we observed a strong colocalization between β-gal (a proxy for GPR37) and the progenitor cell marker Sox2 (~80%) following MCAO (Figure 5a–f). Conversely, only ~40% of all Sox2-positive cells expressed β-gal (Figure 5f), suggesting the existence of different populations of Sox2-positive progenitor cells. Further analyses consequently revealed that the total number of Sox2-positive cells was increased by over two fold (WT: 63 ± 4 (SEM), *Gpr37*$^{-/-}$: 147± 27 (SEM)) within the ischemic core and peri-infarct region of *Gpr37*$^{-/-}$ mice, relative to WT (Figure 5g–i).

Decreased reactivity of oligodendrocyte progenitor cells within *Gpr37*$^{-/-}$ mice

In previous work, we found that *Gpr37*$^{-/-}$ mice exhibited a striking decrease in the normal upregulation of GFAP that is observed after brain injury(30). To more comprehensively explore the role of GPR37 in glial reactivity after stroke-like injury, we assessed changes in the reactive OPC marker NG2 before and after MCAO. Following MCAO in WT mice, NG2-positive glia within the peri-infarct region exhibited a ramified phenotype with strong expression of NG2 (Figure 6b–c), consistent with previous findings by others(41, 42). In contrast, *Gpr37*$^{-/-}$ mice exhibited much more modest expression of NG2 after MCAO, with post-injury intensity of NG2 being significantly reduced, relative to WT mice. (Figure 6e–h). Taken together with our previous findings about reduced GFAP induction in the *Gpr37*$^{-/-}$ mice after MCAO, these data suggest that GPR37 may function as a key regulator of gliosis and the glial microenvironment following brain injury.

DISCUSSION

The present study provides novel evidence for a regulatory role for GPR37 in the modulation of neural stem/progenitor cell (NSPC) dynamics within the peri-infarct zone following cerebral ischemia. We found that GPR37 is dramatically upregulated within a progenitor cell population following the infarct and that deletion of GPR37 consequently altered the dynamics of these cells and surrounding glial cells in response to injury. In the uninjured CNS, GPR37 is predominantly expressed in mature oligodendrocytes, where it functions as a negative regulator of both differentiation and myelination(20). A recent study reported that GPR37 can also be expressed in NSPCs, where it is required for Wnt-dependent neurogenesis(43). Interestingly, following focal ischemia in mice, Wnt-3a administration imparts neuroprotection and functions as a regenerative factor(44). In the present study, we observed that GPR37 expression is not altered within mature oligodendrocytes following stroke but rather dramatically upregulated within Sox2-positive NSPCs where it functions to modulate the presence of these cells within both the ischemic core and peri-infarct region.

The precise origin of the increased Sox2-positive NSPCs in the damaged cortex of mice lacking GPR37 remains unclear. Following stroke, several studies have noted the migration of neuroblasts from the SVZ into the adjacent striatum and cerebral cortex(5, 6, 10). Thus,

it is possible that these cells represent a population of cells that has migrated to the infarct region from a classical stem cell niche such as the SVZ. However, given that these cells are visualized at an acute timepoint following injury and lack staining for the neuroblast marker DCX (Supplemental Figure c), it seems unlikely that these cells represent migrating neuroblasts.

NSPCs have been isolated from numerous regions within the adult mammalian brain(45) and neurogenesis has been reported to occur in atypical brain regions such as the cerebral cortex(46). Although reports are limited, the presence of NSPCs within the ischemia-damaged cortex has previously been demonstrated(10). Moreover, modulation of factors within the injury microenvironment has been found to alter and enhance the dynamics of these cells(10, 11, 47, 48). It is therefore possible that the increased density of Sox2-positive cells within mice lacking GPR37 represents the expansion of a local NSPC niche present within the cortex. Initial studies assessing stroke-induced neurogenesis failed to observe significant neurogenesis within the cerebral cortex, which highlights the general inability of this region to support neurogenesis(5, 6). However, in specific instances neurogenesis could be enhanced through the introduction of growth factors or signaling molecules(48). Our studies provide further evidence by demonstrating that the presence of GPR37 is a key factor regulating the appearance of injury-induced progenitor cells within the cerebral cortex following stroke.

Since most of our analyses were performed three days following stroke, the ultimate fate of the Olig2-positive and Sox2-positive cells, which appear in such large numbers in mice lacking GPR37 after injury, remains unclear. Do these cells go on to commit to the neuronal lineage, or alternatively do they become glial-restricted cells? Future experiments examining longer time points and utilizing fate-restricted mapping could help elucidate the final fate of these progenitors following injury. Another crucial question is whether these cells offer any functional or behavioral benefits to mice lacking GPR37. In a previous study, we performed behavioral assessments 10 days following stroke and found that $Gpr37^{-/-}$ mice recovered from 3-day sensorimotor deficits in both 'time to contact' and 'time to remove' assays, thus suggesting an overall improvement rather than a further deterioration of spatio-motor functions assessed 10 days following stroke(30). Future studies should be targeted at assessing longer time points in order to get a more comprehensive understanding of how alterations in the glial injury environment within $Gpr37^{-/-}$ mice translate to behavioral outcomes associated with stroke recovery.

While it is uncertain whether the loss of GPR37 leads to the increased production of new glial cells, it is evident that following stroke-like injury, GPR37 regulates the activation of existing glial cells Interestingly, recent studies have also highlighted a role for GPR37 in the activation of peripheral macrophages, further suggesting a critical role for this receptor in the modulation of immune responses(49, 50). In a previous study we demonstrated that the loss of GPR37 attenuates astrocyte activation and enhances microglial activation within the injured peri-infarct region following stroke(30). In the present study, we demonstrate that the loss of GPR37 has a pronounced effect on the activation of OPCs following stroke. Since GPR37 is not highly expressed within astrocytes, microglia, or OPCs, it is possible that GPR37 signaling within NSPCs affects the secretion of soluble factors which are capable of

modulating gliosis. Indeed, multiple mechanisms of communication exist between NSPCs and neighboring cells to control various aspects of the injury microenvironment(14, 51, 52). Additionally, the localization of these cells within the ischemic core suggests that within *Gpr37*$^{-/-}$ mice this region may represent an actively regulated region capable of supporting viable cells. To date most stroke research focuses on the peri-infarct region because the ischemic core has generally been classified as a region that has undergone significant necrosis. Interestingly, recent human stroke studies suggest that the cortical ischemic core, but not the peri-infarct region, is a determinant of clinical outcomes following acute ischemic stroke(53, 54).

The downstream signaling pathways and natural ligand for GPR37 remain areas of intense research interest. GPR37 has been reported to bind to and be activated by the secreted protein prosaposin(24, 26, 55) as well as the secreted lipid factor neuroprotectin D1(49). Interestingly, both prosaposin(56–58) and neuroprotectin D1(59–61) have been reported to modulate post-stroke recovery. In our current studies, we examined prosaposin levels in WT vs. *Gpr37*$^{-/-}$ mice following stroke but did not note any significant differences in prosaposin expression (Supplemental Figure F). Future work that clarifies the ligand(s) of GPR37 and the receptor's downstream signaling pathways will shed important light on the roles of GPR37 in modulating CNS responses following stroke.

In summary, our work illustrates a novel role for GPR37 in the regulation of NSPC dynamics following injury and modulation of the glial microenvironment within the post-stroke brain. These findings suggest that GPR37 may be a viable target to enhance the generation of endogenous NSPCs within the injured cortex following ischemic stroke. Additional studies are needed to further assess the effects of GPR37 on neurogenesis and regeneration during chronic phases of stroke.

Supplementary Material

Refer to Web version on PubMed Central for supplementary material.

Acknowledgments:

References:

1. Lo EH, Dalkara T, Moskowitz MA. Mechanisms, challenges and opportunities in stroke. Nat Rev Neurosci. 2003;4(5):399–415. [PubMed: 12728267]

2. Liu YP, Lang BT, Baskaya MK, Dempsey RJ, Vemuganti R. The potential of neural stem cells to repair stroke-induced brain damage. Acta Neuropathol. 2009;117(5):469–80. [PubMed: 19283395]

3. Lindvall O, Kokaia Z. Neurogenesis following Stroke Affecting the Adult Brain. Cold Spring Harb Perspect Biol. 2015;7(11).

4. Lindvall O, Kokaia Z. Stem cells in human neurodegenerative disorders--time for clinical translation? J Clin Invest. 2010;120(1):29–40. [PubMed: 20051634]

5. Arvidsson A, Collin T, Kirik D, Kokaia Z, Lindvall O. Neuronal replacement from endogenous precursors in the adult brain after stroke. Nat Med. 2002;8(9):963–70. [PubMed: 12161747]

6. Parent JM, Vexler ZS, Gong C, Derugin N, Ferriero DM. Rat forebrain neurogenesis and striatal neuron replacement after focal stroke. Ann Neurol. 2002;52(6):802–13. [PubMed: 12447935]

7. Thored P, Arvidsson A, Cacci E, Ahlenius H, Kallur T, Darsalia V, et al. Persistent production of neurons from adult brain stem cells during recovery after stroke. Stem Cells. 2006;24(3):739–47. [PubMed: 16210404]

8. Bonaguidi MA, Stadel RP, Berg DA, Sun J, Ming GL, Song H. Diversity of Neural Precursors in the Adult Mammalian Brain. Cold Spring Harb Perspect Biol. 2016;8(4):a018838. [PubMed: 26988967]

9. Magavi SS, Leavitt BR, Macklis JD. Induction of neurogenesis in the neocortex of adult mice. Nature. 2000;405(6789):951–5. [PubMed: 10879536]

10. Jiang W, Gu W, Brannstrom T, Rosqvist R, Wester P. Cortical neurogenesis in adult rats after transient middle cerebral artery occlusion. Stroke. 2001;32(5):1201–7. [PubMed: 11340234]

11. Zhang R, Xue YY, Lu SD, Wang Y, Zhang LM, Huang YL, et al. Bcl-2 enhances neurogenesis and inhibits apoptosis of newborn neurons in adult rat brain following a transient middle cerebral artery occlusion. Neurobiol Dis. 2006;24(2):345–56. [PubMed: 16996745]

12. Ziv Y, Finkelstein A, Geffen Y, Kipnis J, Smirnov I, Shpilman S, et al. A novel immune-based therapy for stroke induces neuroprotection and supports neurogenesis. Stroke. 2007;38(2 Suppl):774–82. [PubMed: 17261737]

13. Jones DL, Wagers AJ. No place like home: anatomy and function of the stem cell niche. Nat Rev Mol Cell Biol. 2008;9(1):11–21. [PubMed: 18097443]

14. Decimo I, Bifari F, Krampera M, Fumagalli G. Neural stem cell niches in health and diseases. Curr Pharm Des. 2012;18(13):1755–83. [PubMed: 22394166]

15. Jin K, Wang X, Xie L, Mao XO, Zhu W, Wang Y, et al. Evidence for stroke-induced neurogenesis in the human brain. Proc Natl Acad Sci U S A. 2006;103(35):13198–202. [PubMed: 16924107]

16. Minger SL, Ekonomou A, Carta EM, Chinoy A, Perry RH, Ballard CG. Endogenous neurogenesis in the human brain following cerebral infarction. Regen Med. 2007;2(1):69–74. [PubMed: 17465777]

17. Bonfanti L, Peretto P. Adult neurogenesis in mammals--a theme with many variations. Eur J Neurosci. 2011;34(6):930–50. [PubMed: 21929626]

18. Bernstock J. Typical and Atypical Stem Cell Niches of the Adult Nervous System in Health and Inflammatory Brain and Spinal Cord Diseases. 2014.

19. Mu Y, Lee SW, Gage FH. Signaling in adult neurogenesis. Curr Opin Neurobiol. 2010;20(4):416–23. [PubMed: 20471243]

20. Yang HJ, Vainshtein A, Maik-Rachline G, Peles E. G protein-coupled receptor 37 is a negative regulator of oligodendrocyte differentiation and myelination. Nat Commun. 2016;7:10884. [PubMed: 26961174]

21. Marazziti D, Mandillo S, Di Pietro C, Golini E, Matteoni R, Tocchini-Valentini GP. GPR37 associates with the dopamine transporter to modulate dopamine uptake and behavioral responses to dopaminergic drugs. Proc Natl Acad Sci U S A. 2007;104(23):9846–51. [PubMed: 17519329]

22. Morato X, Lujan R, Lopez-Cano M, Gandia J, Stagljar I, Watanabe M, et al. The Parkinson's disease-associated GPR37 receptor interacts with striatal adenosine A2A receptor controlling its cell surface expression and function in vivo. Sci Rep. 2017;7(1):9452. [PubMed: 28842709]

23. Smith BM, Giddens MM, Neil J, Owino S, Nguyen TT, Duong D, et al. Mice lacking Gpr37 exhibit decreased expression of the myelin-associated glycoprotein MAG and increased susceptibility to demyelination. Neuroscience. 2017;358:49–57. [PubMed: 28642167]

24. Giddens MM, Wong JC, Schroeder JP, Farrow EG, Smith BM, Owino S, et al. GPR37L1 modulates seizure susceptibility: Evidence from mouse studies and analyses of a human GPR37L1 variant. Neurobiol Dis. 2017;106:181–90. [PubMed: 28688853]

25. Lundius EG, Stroth N, Vukojevic V, Terenius L, Svenningsson P. Functional GPR37 trafficking protects against toxicity induced by 6-OHDA, MPP+ or rotenone in a catecholaminergic cell line. J Neurochem. 2013;124(3):410–7. [PubMed: 23121049]

26. Lundius EG, Vukojevic V, Hertz E, Stroth N, Cederlund A, Hiraiwa M, et al. GPR37 protein trafficking to the plasma membrane regulated by prosaposin and GM1 gangliosides promotes cell viability. J Biol Chem. 2014;289(8):4660–73. [PubMed: 24371137]

27. Marazziti D, Golini E, Mandillo S, Magrelli A, Witke W, Matteoni R, et al. Altered dopamine signaling and MPTP resistance in mice lacking the Parkinson's disease-associated GPR37/parkin-associated endothelin-like receptor. Proc Natl Acad Sci U S A. 2004;101(27):10189–94. [PubMed: 15218106]

28. Wang HQ, Imai Y, Inoue H, Kataoka A, Iita S, Nukina N, et al. Pael-R transgenic mice crossed with parkin deficient mice displayed progressive and selective catecholaminergic neuronal loss. J Neurochem. 2008;107(1):171–85. [PubMed: 18691389]

29. Zhang X, Mantas I, Fridjonsdottir E, Andren PE, Chergui K, Svenningsson P. Deficits in Motor Performance, Neurotransmitters and Synaptic Plasticity in Elderly and Experimental Parkinsonian Mice Lacking GPR37. Front Aging Neurosci. 2020;12:84. [PubMed: 32292338]

30. McCrary MR, Jiang MQ, Giddens MM, Zhang JY, Owino S, Wei ZZ, et al. Protective effects of GPR37 via regulation of inflammation and multiple cell death pathways after ischemic stroke in mice. FASEB J. 2019;33(10):10680–91. [PubMed: 31268736]

31. Jiang MQ, Zhao YY, Cao W, Wei ZZ, Gu X, Wei L, et al. Long-term survival and regeneration of neuronal and vasculature cells inside the core region after ischemic stroke in adult mice. Brain Pathol. 2017;27(4):480–98. [PubMed: 27514013]

32. Gruttgen A, Reichenzeller M, Junger M, Schlien S, Affolter A, Bosch FX. Detailed gene expression analysis but not microsatellite marker analysis of 9p21 reveals differential defects in the INK4a gene locus in the majority of head and neck cancers. J Pathol. 2001;194(3):311–7. [PubMed: 11439363]

33. Tripathi RB, Jackiewicz M, McKenzie IA, Kougioumtzidou E, Grist M, Richardson WD. Remarkable Stability of Myelinating Oligodendrocytes in Mice. Cell Rep. 2017;21(2):316–23. [PubMed: 29020619]

34. Takebayashi H, Yoshida S, Sugimori M, Kosako H, Kominami R, Nakafuku M, et al. Dynamic expression of basic helix-loop-helix Olig family members: implication of Olig2 in neuron and oligodendrocyte differentiation and identification of a new member, Olig3. Mech Dev. 2000;99(1–2):143–8. [PubMed: 11091082]

35. Zhou Q, Wang S, Anderson DJ. Identification of a novel family of oligodendrocyte lineage-specific basic helix-loop-helix transcription factors. Neuron. 2000;25(2):331–43. [PubMed: 10719889]

36. Lu QR, Yuk D, Alberta JA, Zhu Z, Pawlitzky I, Chan J, et al. Sonic hedgehog--regulated oligodendrocyte lineage genes encoding bHLH proteins in the mammalian central nervous system. Neuron. 2000;25(2):317–29. [PubMed: 10719888]

37. Setoguchi T, Kondo T. Nuclear export of OLIG2 in neural stem cells is essential for ciliary neurotrophic factor-induced astrocyte differentiation. J Cell Biol. 2004;166(7):963–8. [PubMed: 15452140]

38. Ligon KL, Huillard E, Mehta S, Kesari S, Liu H, Alberta JA, et al. Olig2-regulated lineage-restricted pathway controls replication competence in neural stem cells and malignant glioma. Neuron. 2007;53(4):503–17. [PubMed: 17296553]

39. Buffo A, Vosko MR, Erturk D, Hamann GF, Jucker M, Rowitch D, et al. Expression pattern of the transcription factor Olig2 in response to brain injuries: implications for neuronal repair. Proc Natl Acad Sci U S A. 2005;102(50):18183–8. [PubMed: 16330768]

40. Mateo JL, van den Berg DL, Haeussler M, Drechsel D, Gaber ZB, Castro DS, et al. Characterization of the neural stem cell gene regulatory network identifies OLIG2 as a multifunctional regulator of self-renewal. Genome Res. 2015;25(1):41–56. [PubMed: 25294244]

41. Tanaka K, Nogawa S, Ito D, Suzuki S, Dembo T, Kosakai A, et al. Activation of NG2-positive oligodendrocyte progenitor cells during post-ischemic reperfusion in the rat brain. Neuroreport. 2001;12(10):2169–74. [PubMed: 11447328]

42. Levine JM. Increased expression of the NG2 chondroitin-sulfate proteoglycan after brain injury. J Neurosci. 1994;14(8):4716–30. [PubMed: 8046446]

43. Berger BS, Acebron SP, Herbst J, Koch S, Niehrs C. Parkinson's disease-associated receptor GPR37 is an ER chaperone for LRP6. EMBO Rep. 2017;18(5):712–25. [PubMed: 28341812]

44. Wei ZZ, Zhang JY, Taylor TM, Gu X, Zhao Y, Wei L. Neuroprotective and regenerative roles of intranasal Wnt-3a administration after focal ischemic stroke in mice. J Cereb Blood Flow Metab. 2018;38(3):404–21. [PubMed: 28430000]

45. Gage FH. Mammalian neural stem cells. Science. 2000;287(5457):1433–8. [PubMed: 10688783]

46. Gould E, Reeves AJ, Graziano MS, Gross CG. Neurogenesis in the neocortex of adult primates. Science. 1999;286(5439):548–52. [PubMed: 10521353]

47. Leker RR, Soldner F, Velasco I, Gavin DK, Androutsellis-Theotokis A, McKay RD. Long-lasting regeneration after ischemia in the cerebral cortex. Stroke. 2007;38(1):153–61. [PubMed: 17122419]

48. Kolb B, Morshead C, Gonzalez C, Kim M, Gregg C, Shingo T, et al. Growth factor-stimulated generation of new cortical tissue and functional recovery after stroke damage to the motor cortex of rats. J Cereb Blood Flow Metab. 2007;27(5):983–97. [PubMed: 16985505]

49. Bang S, Xie YK, Zhang ZJ, Wang Z, Xu ZZ, Ji RR. GPR37 regulates macrophage phagocytosis and resolution of inflammatory pain. J Clin Invest. 2018;128(8):3568–82. [PubMed: 30010619]

50. Bang S, Donnelly CR, Luo X, Toro-Moreno M, Tao X, Wang Z, et al. Activation of GPR37 in macrophages confers protection against infection-induced sepsis and pain-like behaviour in mice. Nat Commun. 2021;12(1):1704. [PubMed: 33731716]

51. Morrison SJ, Spradling AC. Stem cells and niches: mechanisms that promote stem cell maintenance throughout life. Cell. 2008;132(4):598–611. [PubMed: 18295578]

52. Willis CM, Nicaise AM, Hamel R, Pappa V, Peruzzotti-Jametti L, Pluchino S. Harnessing the Neural Stem Cell Secretome for Regenerative Neuroimmunology. Front Cell Neurosci. 2020;14:590960. [PubMed: 33250716]

53. Koennecke HC. Editorial comment--Challenging the concept of a dynamic penumbra in acute ischemic stroke. Stroke. 2003;34(10):2434–5. [PubMed: 14500920]

54. Jovin TG, Yonas H, Gebel JM, Kanal E, Chang YF, Grahovac SZ, et al. The cortical ischemic core and not the consistently present penumbra is a determinant of clinical outcome in acute middle cerebral artery occlusion. Stroke. 2003;34(10):2426–33. [PubMed: 14500935]

55. Liu B, Mosienko V, Vaccari Cardoso B, Prokudina D, Huentelman M, Teschemacher AG, et al. Glio- and neuro-protection by prosaposin is mediated by orphan G-protein coupled receptors GPR37L1 and GPR37. Glia. 2018;66(11):2414–26. [PubMed: 30260505]

56. Morita F, Wen TC, Tanaka J, Hata R, Desaki J, Sato K, et al. Protective effect of a prosaposin-derived, 18-mer peptide on slowly progressive neuronal degeneration after brief ischemia. J Cereb Blood Flow Metab. 2001;21(11):1295–302. [PubMed: 11702044]

57. Lu AG, Otero DA, Hiraiwa M, O'Brien JS. Neuroprotective effect of retro-inverso Prosaptide D5 on focal cerebral ischemia in rat. Neuroreport. 2000;11(8):1791–4. [PubMed: 10852246]

58. Igase K, Tanaka J, Kumon Y, Zhang B, Sadamoto Y, Maeda N, et al. An 18-mer peptide fragment of prosaposin ameliorates place navigation disability, cortical infarction, and retrograde thalamic degeneration in rats with focal cerebral ischemia. J Cereb Blood Flow Metab. 1999;19(3):298–306. [PubMed: 10078882]

59. Belayev L, Mukherjee PK, Balaszczuk V, Calandria JM, Obenaus A, Khoutorova L, et al. Neuroprotectin D1 upregulates Iduna expression and provides protection in cellular uncompensated oxidative stress and in experimental ischemic stroke. Cell Death Differ. 2017;24(6):1091–9. [PubMed: 28430183]

60. Yao C, Zhang J, Chen F, Lin Y. Neuroprotectin D1 attenuates brain damage induced by transient middle cerebral artery occlusion in rats through TRPC6/CREB pathways. Mol Med Rep. 2013;8(2):543–50. [PubMed: 23799606]

61. Bazan NG, Eady TN, Khoutorova L, Atkins KD, Hong S, Lu Y, et al. Novel aspirin-triggered neuroprotectin D1 attenuates cerebral ischemic injury after experimental stroke. Exp Neurol. 2012;236(1):122–30. [PubMed: 22542947]
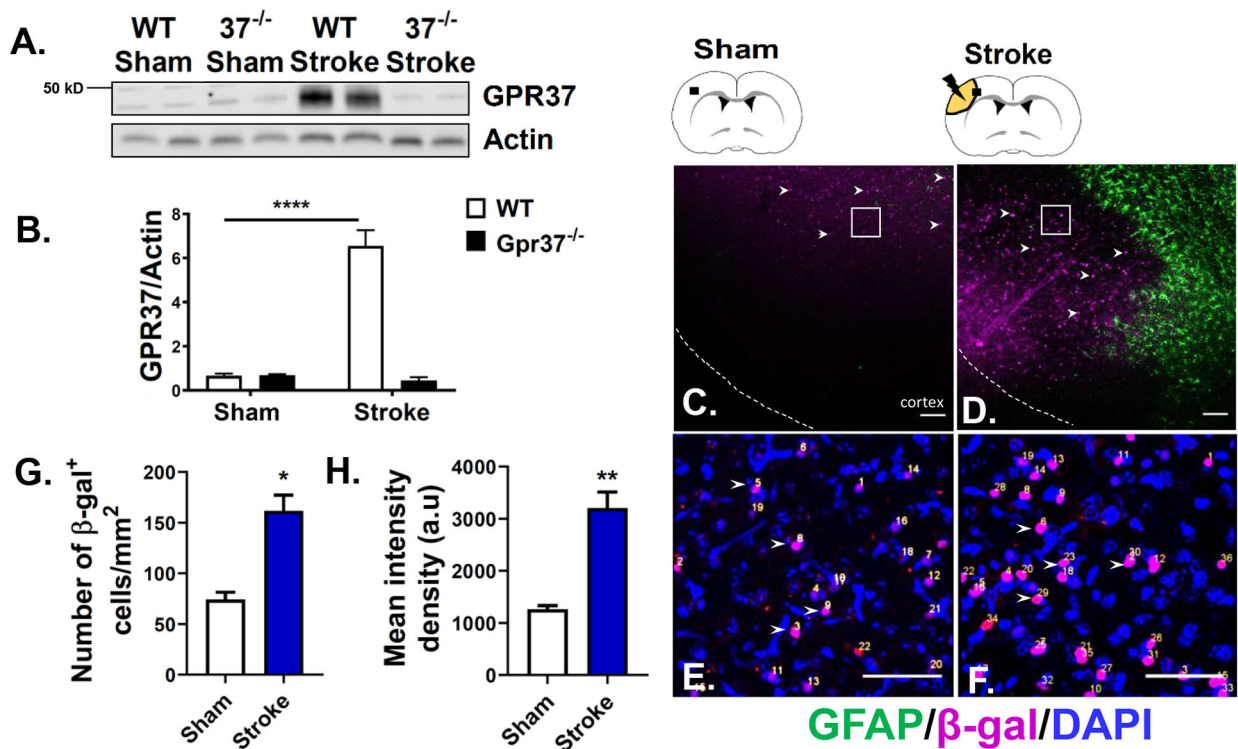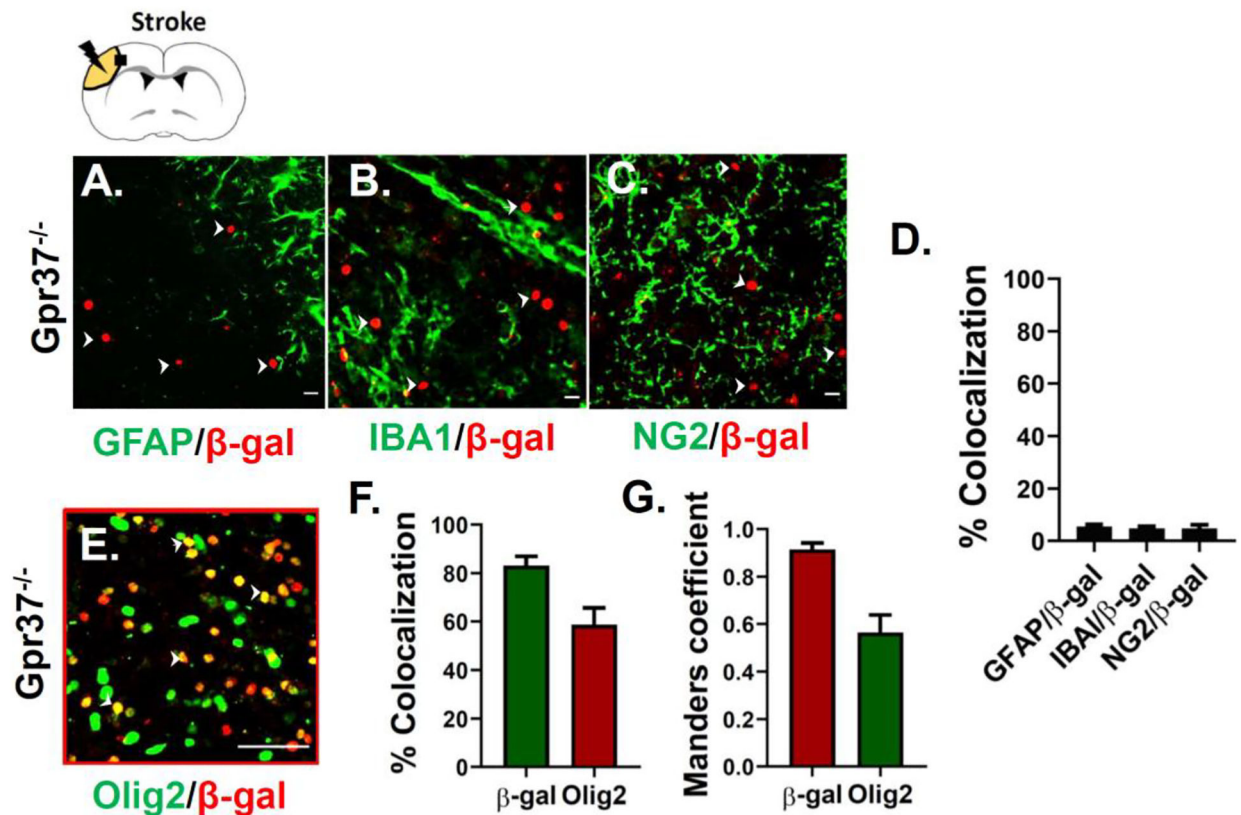
Figure 1. GPR37 is upregulated following ischemic injury.
(a) Representative Western blot of GPR37 levels within the penumbra region of WT and Gpr37$^{-/-}$ mice following MCAO and within an analogous region in sham controls. (b) Quantification of the data shown in panel A. Bars represent mean ± SEM, N=4, two-way ANOVA (Holm-Sidak), *p<0.05, ****p<0.0001. (c) Immunohistochemical staining depicting β-gal+ cells within the cortex of *Gpr37*$^{-/-}$ sham mice and (d) Analogous peri-infarct region within a Gpr37$^{-/-}$ MCAO brain. e) Magnified zoom of white box depicted in panel C. (f) Magnified zoom of white box depicted in panel D. (g) Quantification of β-gal+ cells within the cortex/peri-infarct region of *Gpr37*$^{-/-}$ sham and MCAO brains. (h) Quantification of mean intensity density of β-gal+ cells within the cortex/penumbra of sham and *Gpr37*$^{-/-}$ MCAO brains. Bars represent mean ± SEM, N=4–6, t-test, *p<0.05**p<0.01. White arrowheads represent β-gal+ cells. The white dashed line represents the tissue boundary. Scale bars in panels C and D represent 100 μm. Scale bars in panels E and F represent 50 μm.
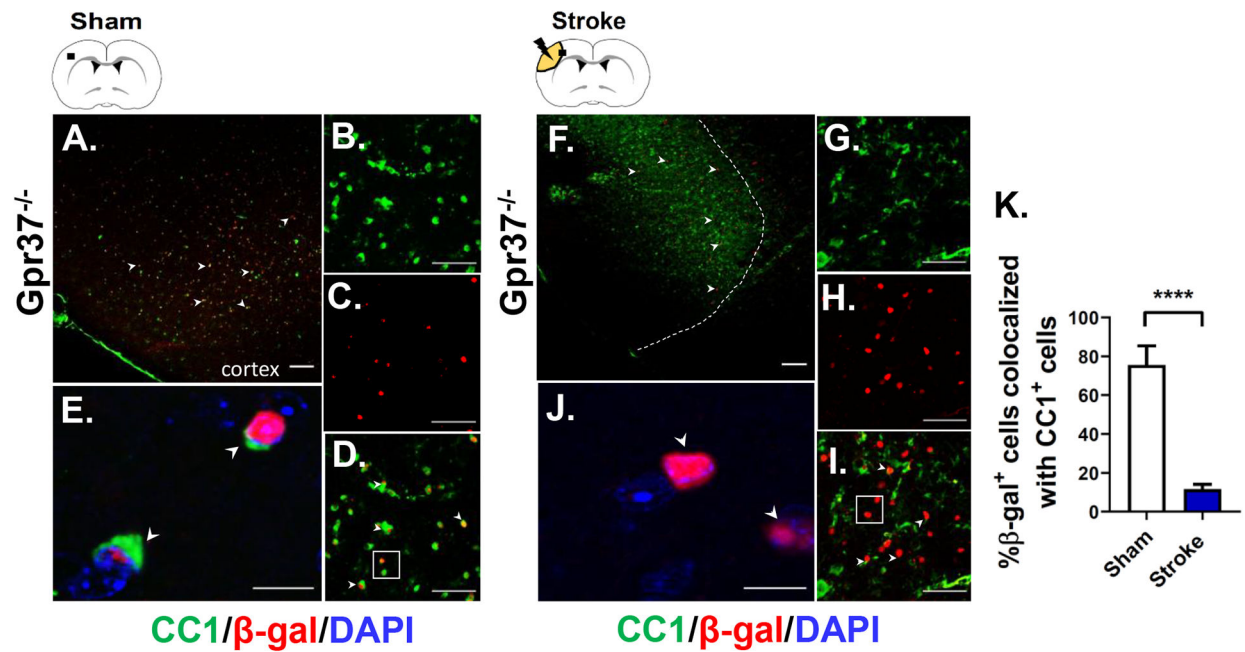
Figure 2. Post-stroke Gpr37-positive cells are not mature oligodendrocytes.
Immunolabeling depicting β-gal+/CC1+ cells within the cortical region of sham brains (a-e) and stroke peri-infarct region (f-i) 72 hrs following MCAO. The white dashed line represents the boundary of the ischemic core (e) Magnified zoom of sham region image shown in panel D. (j) Magnified zoom of peri-infarct region shown in panel I. (k) Quantification of the percentage of β-gal+ cells colocalized with CC1+ cells within the cortex of Gpr37$^{-/-}$ sham brains and penumbra of stroke brains. White arrowheads represent β-gal+ cells. Bars represent mean ± SEM, N=4–6, t-test, ****p<0.0001. Scale bar=100 μm (A and F). Scale bar=50 μm (B, C, D, G, H, and I). Scale bars=10 μm (E and J).
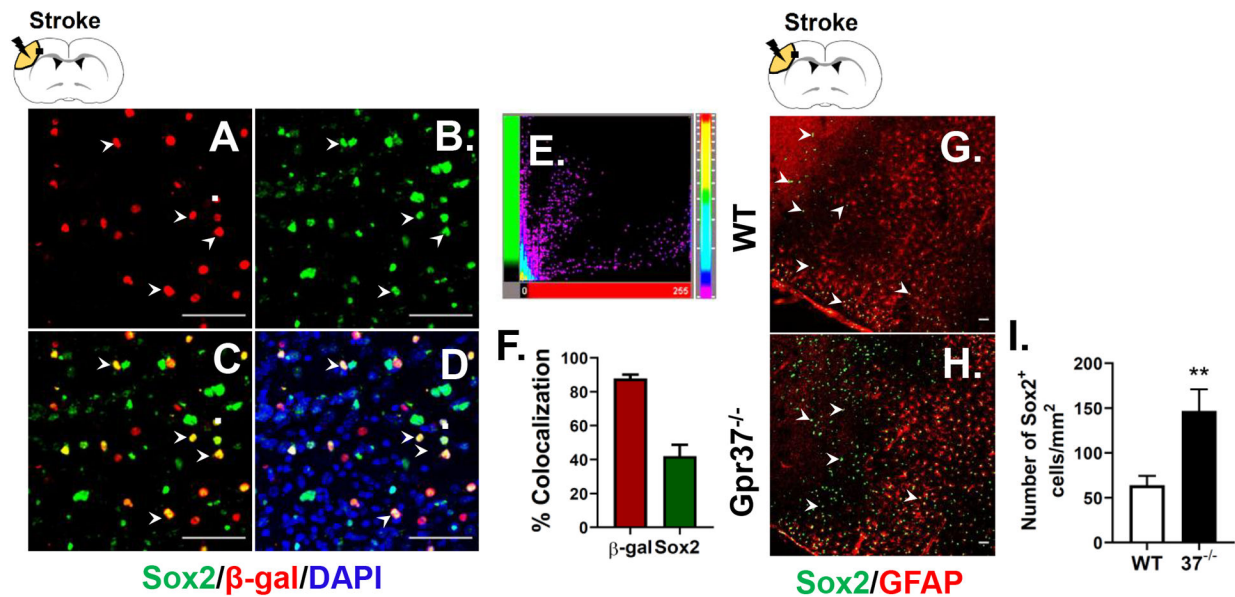
Figure 3. GPR37 is upregulated in Olig2-positive cells but not reactive glia following stroke.
(a-c) Immunolabeling within the penumbra of *Gpr37*^{−/−} mice 72hrs following MCAO. A lack of colocalization was observed between β-gal+ cells and GFAP+ reactive astrocytes (a), IBA1+ reactive microglia (b) and NG2+ OPCs (c). (d) Quantification of the percent colocalization between β-gal and the markers depicted in panels A-C. (e) Immunohistochemical staining depicting a high degree of colocalization between β-gal+ cells and Olig2+ cells within the penumbra 72hrs following MCAO. White arrowheads indicate β-gal+ cells. (f) Quantification of the percent colocalization between Olig2-positive and β-gal-positive cells following stroke. (g) Analysis of Mander's coefficient of the colocalization shown in panel E. Scale bars=10 μm (A, B, and C). Scale bar=50 μm (E).
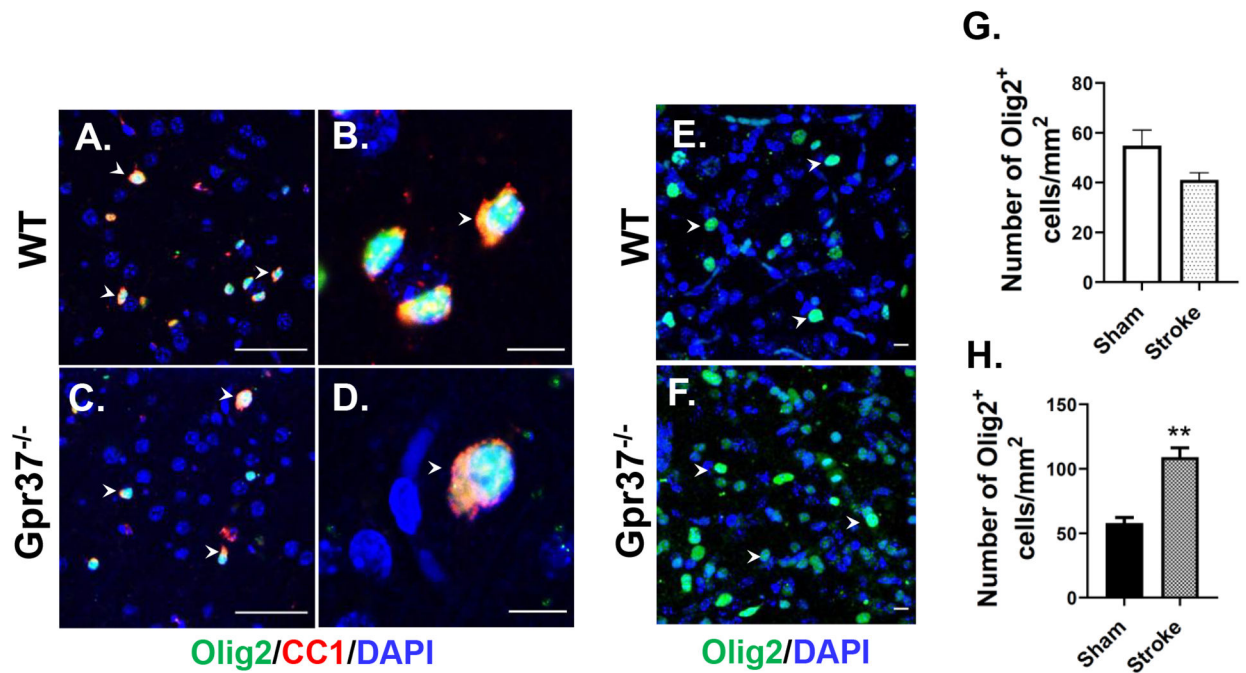
Figure 4. Olig2-positive cells are upregulated within the penumbra of Gpr37$^{-/-}$ mice.
(a) Immunolabeling of the cortical region of WT brains using antibodies against Olig2 and CC1. (b) Magnified zoom of panel a. (c) Immunolabeling of the cortical region of *Gpr37*$^{-/-}$ sham brains using antibodies against Olig2 and CC1. (d) Magnified zoom of panel c. (e) Immunolabeling of Olig2+ cells within cortical regions of WT and (f) *Gpr37*$^{-/-}$ stroke penumbra region. White arrowheads represent Olig2+ cells (g) Quantification of WT data shown in panels a and e, (h) Quantification of *Gpr37*$^{-/-}$ data shown in panels b and f. Bars represent mean ± SEM, N=4–6, t-test, **p<0.01. Scale bar=50μm (A and C). Scale bar=10 μm (B,D,E-F).

Figure 5. GPR37 is upregulated within Sox2-positive progenitor cells and alters their dynamics within the injury zone.

Immunolabeling within the penumbra of *Gpr37*$^{-/-}$ mice 72 hrs. following MCAO. Colocalization was observed between β-gal+ cells and Sox2+ cells (a-d). White arrowheads represent β-gal+ /Sox2+cells (e) Scatter plot of the colocalization distribution between β-gal+ and Sox2+ cells within the penumbra. (f) Quantification of the percent of colocalization between Olig2+ and β-gal+ cells following stroke (~80% of β-gal+ cells were Sox2+, whereas ~40% of Sox2+ cells were β-gal+. (g) Immunolabeling of Sox2+ cells within the peri infarct of WT mice 72 hrs following MCAO. (h) Immunolabeling of Sox2+ cells within the peri infarct of *Gpr37*$^{-/-}$ mice 72 hrs following MCAO. Reactive astrocytes are labelled using GFAP. White arrowheads represent Sox2+ cells. (i) Quantification of the number of Sox2+ cells within the peri infarct region of WT and *Gpr37*$^{-/-}$ mice following MCAO. Bars represent mean ± SEM, N=4–6. Scale bar=50μm.
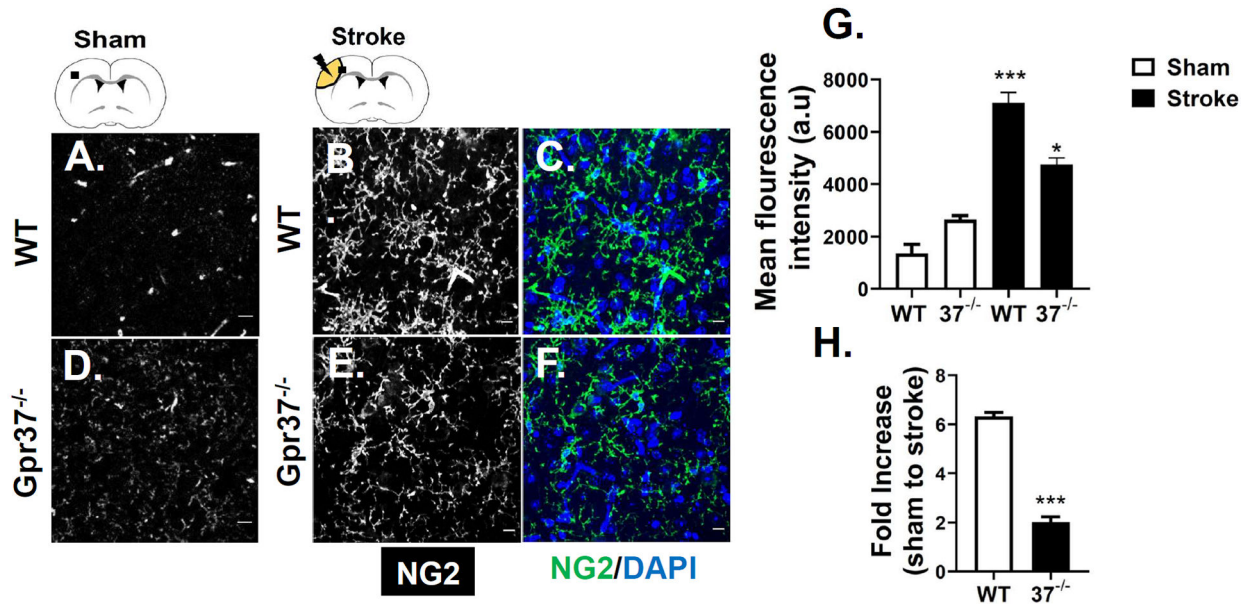
Figure 6. Loss of GPR37 impairs OPC activation following injury.
Immunolabeling of NG2+ cells within the uninjured cortical region of WT (a) and Gpr37$^{-/-}$ sham (d) and the injured penumbra of WT (b-c) and *Gpr37*$^{-/-}$ mice (e-f) following MCAO. (c) Panel b shown with corresponding DAPI staining. (g) Panel f shown with corresponding DAPI staining; NG2 labeling is depicted in green. (g-h) Quantification of mean fluorescence intensity and the fold increase in intensity for WT and *Gpr37*$^{-/-}$ data shown in panels a-f. In panel g, bars represent mean ± SEM, N=4–6, one-way ANOVA (Holm-Sidak), *p<0.05, ***p<0.001. In panel h, bars represent mean ± SEM, N=4–6, t-test, *p<0.05. f. Scale bar=10μm.